Comparing Exact and Generalized Regression Neural Network Solutions for Free Vibration of Elastically Supported Timoshenko Beams with Attached Masses

Bülent Yıldırım[a] and Oktay Demirdağ[b]

[a] Pamukkale University, Engineering Faculty, Civil Engineering Department,
20070 Kınıklı, Denizli, Turkey.
Email: byildirim@pau.edu.tr

[b] Corresponding author. Pamukkale University, Engineering Faculty, Civil Engineering Department,
20070 Kınıklı, Denizli, Turkey.
Email: oktaydemirdag@pau.edu.tr

Abstract
In this study, as the Artificial Neural Networks (ANN) is becoming increasingly common in the modeling and forecasting in many disciplines of engineering, Generalized Regression Neural Networks (GRNN) model is used to obtain natural frequencies of elastically supported Timoshenko beams with attached masses and the obtained frequencies are compared with the frequencies obtained from the exact solution of the same beam model. The elastically supported cantilever Timoshenko beam carrying multiple attached masses with rotary inertia is chosen as a mathematical model. The concept of fixity factor is used to define the stiffness of the elastic support. The governing equation of the beam elements is solved by applying the separation of variables method in the transfer matrix method (TMM) algorithm that gives the exact solution. The data used in the training, testing and verification phases of GRNN are obtained from TMM. The comparison graphs are presented for training, testing and verification data in numerical analysis to show the effectiveness of the GRNN, and it is resulted that neural network approach gives close results to TMM in training and testing phases.

Keywords: Free Vibration; Timoshenko Beam; Attachments with Rotary Inertia; Transfer Matrix; Generalized Regression Neural Network.

1. Introduction

Artificial neural networks (ANN) have been recently accepted as an efficient alternative tool for modeling of some complex engineering systems and widely used for forecasting. Some specific applications of ANN to beam vibration include vibration and stability of axially moving beams (Özkaya and Öz 2002), vibration of beam-mass systems (Karlık et al 1998; Özkaya and Pakdemirli 1999) and vibration control (Allı et al 2003). GRNN method has also been used for many specific studies (Kim et al 2004; Cigizoglu and Alp 2005; Ramadhas et al 2006; Celikoglu 2006; Celikoglu and Cigizoglu 2007).

Vibration of Timoshenko beams (Esmailzadeh and Ohadi 2000; Ruta 2006; Ferreira and Fasshauer 2006; Lee et al 2004) and vibration of beams with attachments (Karami et al 2003; Posiadala 1997; Gökdağ and Kopmaz 2005; Özkaya 2002; Wu and Chiang 2004; Wu 2006; Wu and Chen 2001; Rao et al 2006; Salarieh and Ghorashi 2006) are considered in many studies. TMM is used with Holzer method for torsional vibration of systems with concentrated masses (Hurty and Rubinstein 1964), and with Myklestad-Thomson method for flexural vibrations of discrete systems with concentrated masses (Thomson 1981). TMM is used for also transverse vibration of beams with attachments (Bapat and Bapat 1987; Lin and Chang 2005).

The main purpose of this study is to investigate the applicability and capability of ANN approach for vibration frequency forecasting. To verify the application of this approach, free vibration analysis of elastically supported Timoshenko beam with attached masses with rotary inertias is made by TMM for. The criteria of performance evaluation are calculated to evaluate the performances of the GRNN models. The frequency estimation models having various input structures are constructed to investigate the applicability of GRNN method. The estimation models are trained and tested by GRNN method for three cross validation training and testing sets. The results of GRNN models for training, testing and are evaluated. Moreover GRNN estimation models are also verified by verification data set and the results of models are compared. The results of training and testing demonstrate that GRNN can be successfully applied and provide high accuracy and reliability for natural frequency forecasting for a beam with attachments.
Many researchers investigate the vibration of beam-columns with attached masses using conventional methods, most of them requiring much computing effort and time. In this study, two approaches having different characteristics, one being TMM that gives exact solution by decreasing computational effort and time by reducing the dimension of the considered matrix to four for all problems, and the other being neural network approach that again needs less computational effort and time.

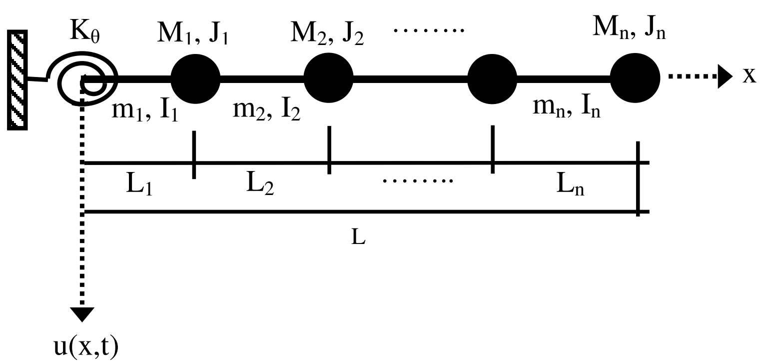

Fig. 1. Elastically supported Timoshenko beam with attached masses

1.1. Problem Definition

The mathematical model of n uniform Timoshenko beams with n attached masses given in Fig. 1 is used in this study. Elastic support is modeled by rotation spring. In order to reflect the relative stiffness of the beam and the rotational spring an end fixity factor is defined. Thus, the fixity factor is defined in Eq. (1) from the rotational stiffness so that it takes as limits: null (0) value for a theoretically pinned joint and unity (1) for a theoretically rigid one (Cabrero and Bayo 2005).

$$f = \frac{1}{1 + \dfrac{3EI}{K_\theta L}} \qquad (0 \leq f \leq 1) \qquad (1)$$

where EI and L are flexural rigidity and length of the Timoshenko beam, K_θ is the rotational spring constant. The governing equation of the free vibration is derived by including bending and shear deformation with rotary inertia of the beams. The rotary inertia of the attached masses is also included in the analysis. In order to study with nondimensionalized values the multiplication factors are defined for attached mass and its rotary inertia, respectively, as in the following

$$\overline{M}_i = \frac{M_i}{m_i L_i} \qquad \overline{J}_i = \frac{L_i}{m_i L_i^3} \tag{2}$$

where M_i and J_i are ith attached mass and its rotary inertia, L_i is the length of ith beam. In this study, the natural frequencies of the model having different number of attached masses are obtained by three algorithms considering the variation of fixity factor, nondimensionalized attached mass and its rotary inertia values. Firstly, a TMM approach considering the continuity relations of displacement, slope, moment and shear at the interface of adjacent beams is performed to determine eigenfrequencies of the model. Considering the compatibility conditions at the interface of adjacent beams the relations between two adjacent spans is obtained; thus, exact values of eigenfrequencies of the entire system are determined for different number of masses by using TMM algorithm. ANN algorithm is the second method used to obtain the frequencies of the model for the same conditions by using GRNN model. The number of attached masses, nondimensionalized attached mass and its rotary inertia values, and fixity factors are the four inputs and the natural frequencies are the outputs necessary for the GRNN algorithm.

1.2. Artificial Neural Networks

A neural network consists of a large number of simple processing elements, called neuron. Generally an ANN, can be defined as a system or mathematical model which consists of many nonlinear artificial neurons running in parallel which may be generated as one layered or multiple layered. The most ANN has three layers: input, output and hidden layers. Input layer is used to present the input data to the network and output layer is used to get the response of network. Hidden layer, located between input and output layer, is used to process the nonlinear mathematical. In literature, there are many types of ANN such as Feed Forward Neural Networks (FFNN), Radial Basis Neural Networks and Generalized Regression Neural Networks (GRNN) etc. In this study, the GRNN method is used to estimate the natural frequencies of a vibrating beam. The frequency estimation models having various input structures are constructed to investigate the applicability of GRNN method. The estimation models are trained and tested by GRNN method for three cross validation training and testing sets. The results of GRNN models for training, testing and are evaluated. Moreover GRNN estimation models are also verified by verification data set and the results of models are compared. The results demonstrate that GRNN can be successfully applied and provide high accuracy and reliability in training and testing phases for natural frequency forecasting for a beam with attachments.

2. Analysis by TMM

2.1. Determining Eigenfunction

Differential equation of motion for the ith Timoshenko beam is

$$\frac{\partial^4 u_i}{\partial x_i^4} - \left(\frac{m_i k_i}{AG_i} + \frac{m_i r_i^2}{EI_i} \right) \frac{\partial^4 u_i}{\partial x_i^2 \partial t^2} + \frac{m_i^2 r_i^2 k_i}{EI_i AG_i} \frac{\partial^4 u_i}{\partial t^4} + \frac{m_i}{EI_i} \frac{\partial^2 u_i}{\partial t^2} = 0 \tag{3}$$

where $u_i(x_i,t)$, m_i, r_i, k_i, EI_i and AG_i, are displacement at x_i ($0 \le x_i \le L_i$), distributed mass, radius of gyration, effective shear area factor due to cross-section geometry, flexural and shear rigidities, respectively, of the ith beam. Applying the separation of variables method to Eq. (3) in the form of Eq. (4) for $T(t) \neq 0$ and rearranging with the dimensionless parameters gives the eigenfunction $X(x_i)$ of the ith beam as in Eq. (5).

$$u_i(x_i,t) = X_i(x_i)T(t) = X_i(x_i)\left[A\sin(\omega t) + B\cos(\omega t)\right] \quad (4)$$

$$X_i(x_i) = C_{1i}\sinh(\lambda_{1i}x_i) + C_{2i}\cosh(\lambda_{1i}x_i) + C_{3i}\sin(\lambda_{2i}x_i) + C_{4i}\cos(\lambda_{2i}x_i) \quad (5)$$

Where, $\alpha_{1i} = m_i k_i \omega^2 / AG_i$; $\alpha_{2i} = m_i\omega^2 / EI_i$; $\alpha_{3i} = \alpha_{1i} + \alpha_{2i}r_i^2$;

$\Delta_i = \left(\alpha_{1i} - \alpha_{2i}r_i^2\right)^2 + 4\alpha_{2i}$; $n_{1i} = \left(-\alpha_{3i} + \sqrt{\Delta_i}\right)/2$; $n_{2i} = \left(-\alpha_{3i} - \sqrt{\Delta_i}\right)/2$; $\lambda_{1i} = \sqrt{n_{1i}}$; $\lambda_{2i} = \sqrt{|n_{2i}|}$;

$C_{1i}...C_{4i}$ are integration constants. Moment, shear, slope functions of the ith Timoshenko beam are (Tuma and Cheng 1983).

$$M_i(x_i,t) = -EI_i u_i''(x_i,t) - EI_i\alpha_1 u_i(x_i,t) \quad (6.1)$$

$$V_i(x_i,t) = \left[-EI_i/\left(1-\alpha_{1i}r_i^2\right)\right]\left[u_i'''(x_i,t) + \alpha_{3i}u_i'(x_i,t)\right] \quad (6.2)$$

$$\theta_i(x_i,t) = u_i'(x_i,t) - V_i(x_i,t)k_i / AG_i \quad (6.3)$$

2.2. Boundary Conditions

Boundary conditions at the interface of the adjacent (i-1)th and ith beams (Fig. 2) are written as in Eq. (7) using the continuity of displacement and slope and the equilibrium of moment and shear.

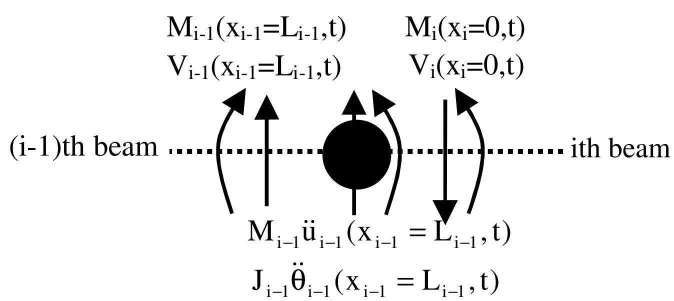

Fig. 2. Free body diagram for the interface of (i-1)th and (i)th beams

$$u_{i-1}(x_{i-1}=L_{i-1},t) = u_i(x_i=0,t) \quad (7.1)$$

$$\theta_{i-1}(x_{i-1}=L_{i-1},t) = \theta_i(x_i=0,t) \quad (7.2)$$

$$M_{i-1}(x_{i-1}=L_{i-1},t) - J_{i-1}\ddot{\theta}_{i-1}(x_{i-1}=L_{i-1},t) = M_i(x_i=0,t) \quad (7.3)$$

$$V_{i-1}(x_{i-1}=L_{i-1},t) + M_{i-1}\ddot{u}_{i-1}(x_{i-1}=L_{i-1},t) = V_i(x_i=0,t) \quad (7.4)$$

Since continuity of displacement and slope is not valid for the support and the nth attached mass, one gets 4(n-1) relations from Eq. (7). However, four more relations are needed for the entire system, two given in Eq. (8) from the elastic support in Fig. 3 and two given in Eq. (9) from the nth attached mass in Fig. 4 where K_θ is rotational spring constant.

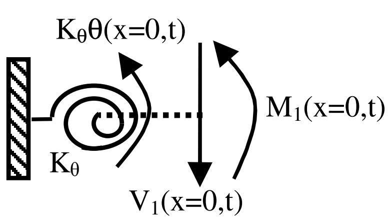

Fig. 3. Free body diagram of elastic support of the beam

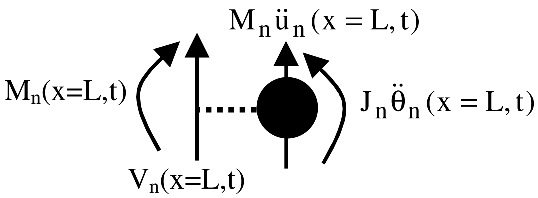

Fig. 4. Free body diagram of (n)th mass on the beam

$$\left.\begin{aligned} & u_1(x_1 = 0, t) = 0 \\ & M_1(x_1 = 0, t) = -K_\theta \theta_1(x_1 = 0, t) \end{aligned}\right\} \tag{8}$$

$$\left.\begin{aligned} & M_n(x_n = L_n, t) = J_n \ddot{\theta}_n(x_n = L_n, t) \\ & V_n(x_n = L_n, t) = -M_n \ddot{u}_n(x_n = L_n, t) \end{aligned}\right\} \tag{9}$$

2.3. Obtaining Transfer Matrix

The relation between $C_{1i} \ldots C_{4i}$ and $C_{1i-1} \ldots C_{4i-1}$ is written from Eq. (7) in matrix form as

$$\begin{Bmatrix} C_{1i} \\ C_{2i} \\ C_{3i} \\ C_{4i} \end{Bmatrix} = [T_i] \begin{Bmatrix} C_{1i-1} \\ C_{2i-1} \\ C_{3i-1} \\ C_{4i-1} \end{Bmatrix} = \begin{bmatrix} T_{i11} & T_{i12} & T_{i13} & T_{i14} \\ T_{i21} & T_{i22} & T_{i23} & T_{i24} \\ T_{i31} & T_{i32} & T_{i33} & T_{i34} \\ T_{i41} & T_{i42} & T_{i43} & T_{i44} \end{bmatrix} \begin{Bmatrix} C_{1i-1} \\ C_{2i-1} \\ C_{3i-1} \\ C_{4i-1} \end{Bmatrix} \text{(i=2,3,…,n)} \tag{10}$$

where $T_{i11} = \alpha_{26i}\alpha_{9i-1}ch_{i-1} + \alpha_{27i}\alpha_{14i-1}$; $T_{i12} = \alpha_{26i}\alpha_{9i-1}sh_{i-1} + \alpha_{27i}\alpha_{15i-1}$;

$T_{i13} = \alpha_{26i}\alpha_{10i-1}c_{i-1} + \alpha_{27i}\alpha_{16i-1}$; $T_{i14} = -\alpha_{26i}\alpha_{10i-1}s_{i-1} + \alpha_{27i}\alpha_{17i-1}$; $T_{i21} = \alpha_{31i}sh_{i-1} - \alpha_{30i}\alpha_{21i-1}$;

$T_{i22} = \alpha_{31i}ch_{i-1} - \alpha_{30i}\alpha_{22i-1}$; $T_{i23} = \alpha_{31i}s_{i-1} - \alpha_{30i}\alpha_{23i-1}$; $T_{i24} = \alpha_{31i}c_{i-1} - \alpha_{30i}\alpha_{24i-1}$;

$T_{i31} = \alpha_{28i}\alpha_{9i-1}ch_{i-1} - \alpha_{29i}\alpha_{14i-1}$; $T_{i32} = \alpha_{28i}\alpha_{9i-1}sh_{i-1} - \alpha_{29i}\alpha_{15i-1}$;

$T_{i33} = \alpha_{28i}\alpha_{10i-1}c_{i-1} - \alpha_{29i}\alpha_{16i-1}$; $T_{i34} = -\alpha_{28i}\alpha_{10i-1}s_{i-1} - \alpha_{29i}\alpha_{17i-1}$; $T_{i41} = \alpha_{32i}sh_{i-1} + \alpha_{30i}\alpha_{21i-1}$;

$T_{i42} = \alpha_{32i}ch_{i-1} + \alpha_{30i}\alpha_{22i-1}$; $T_{i43} = \alpha_{32i}s_{i-1} + \alpha_{30i}\alpha_{23i-1}$; $T_{i44} = \alpha_{32i}c_{i-1} + \alpha_{30i}\alpha_{24i-1}$;

$\alpha_{32i} = \alpha_{4i}\alpha_{30i}$; $\alpha_{31i} = \alpha_{5i}\alpha_{30i}$; $\alpha_{30i} = 1/(\alpha_{4i} + \alpha_{5i})$; $\alpha_{29i} = \alpha_{9i}/\alpha_{25i}$; $\alpha_{28i} = \alpha_{12i}/\alpha_{25i}$;

$\alpha_{27i} = \alpha_{10i}/\alpha_{25i}$; $\alpha_{26i} = \alpha_{13i}/\alpha_{25i}$; $\alpha_{25i} = \alpha_{9i}\alpha_{13i} + \alpha_{12i}\alpha_{10i}$; $\alpha_{24i} = \alpha_{5i}c_i - \alpha_{20i}s_i$;

$\alpha_{23i} = \alpha_{5i}s_i + \alpha_{20i}c_i$; $\alpha_{22i} = \alpha_{19i}sh_i - \alpha_{4i}ch_i$; $\alpha_{21i} = \alpha_{19i}ch_i - \alpha_{4i}sh_i$; $\alpha_{20i} = \alpha_{18i}\alpha_{10i}$;

$\alpha_{19i} = \alpha_{18i}\alpha_{9i}$; $\alpha_{18i} = J_i\omega^2$; $\alpha_{17i} = \alpha_{13i}s_i - \alpha_{11i}c_i$;

$\alpha_{16i} = -\alpha_{13i}c_i - \alpha_{11i}s_i$; $\alpha_{15i} = \alpha_{12i}sh_i - \alpha_{11i}ch_i$; $\alpha_{14i} = \alpha_{12i}ch_i - \alpha_{11i}sh_i$; $\alpha_{13i} = \alpha_{6i}\alpha_{8i}$; $\alpha_{12i} = \alpha_{6i}\alpha_{8i}$;

$\alpha_{11i} = M_i\omega^2$; $\alpha_{10i} = \lambda_{2i} + \alpha_{6i}\alpha_{8i}k_i/AG_i$; $\alpha_{9i} = \lambda_{1i} - \alpha_{6i}\alpha_{7i}k_i/AG_i$; $\alpha_{8i} = \lambda_{2i}(\lambda_{2i}^2 - \alpha_{3i})$;

$\alpha_{7i} = \lambda_{1i}(\lambda_{1i}^2 + \alpha_{3i})$; $\alpha_{6i} = -EI_i/(1 - \alpha_{1i}r_i^2)$; $\alpha_{5i} = EI_i(\lambda_{2i}^2 - \alpha_{1i})$; $\alpha_{4i} = EI_i(\lambda_{1i}^2 + \alpha_{1i})$ $sh_i = \sinh(\lambda_{1i}L_i)$;

$ch_i = \cosh(\lambda_{1i}L_i)$; $s_i = \sin(\lambda_{2i}L_i)$; $c_i = \cos(\lambda_{2i}L_i)$

Applying Eq. (10) consecutively for n beam segment gives

$$\begin{Bmatrix} C_{1n} \\ C_{2n} \\ C_{3n} \\ C_{4n} \end{Bmatrix} = [T_t]\begin{Bmatrix} C_{11} \\ C_{21} \\ C_{31} \\ C_{41} \end{Bmatrix} = [T_n][T_{n-1}]....[T_3][T_2]\begin{Bmatrix} C_{11} \\ C_{21} \\ C_{31} \\ C_{41} \end{Bmatrix} \tag{11}$$

where $[T_t]$ is the transfer matrix of the entire system. Substituting Eq. (11) into Eq. (9) gives two more equation related to $C_{11}\ldots C_{41}$, therefore, there exists 4 homogeneous equations together with Eq. (8) that characterize free vibration of the entire system as

$$[F]\begin{Bmatrix} C_{11} \\ C_{21} \\ C_{31} \\ C_{41} \end{Bmatrix} = \begin{Bmatrix} 0 \\ 0 \\ 0 \\ 0 \end{Bmatrix} \tag{12}$$

where [F] is coefficient matrix. Equating the determinant of [F] to zero gives frequency equation of the entire system, and every root of this frequency equation is the eigenfrequency of the model. These frequencies are computed by a program written by the author considering the secant method (Low 1991).

3. Analysis by GRNN

A Generalized Regression Neural Networks (GRNN) is a variation of the radial basis neural networks, which is based on kernel regression networks (Cigizoglu and Alp 2005). A GRNN doesn't require an iterative training procedure as back propagation networks. A GRNN consists of four layers: input layer, pattern layer, summation layer and output layer (Fig. 5).

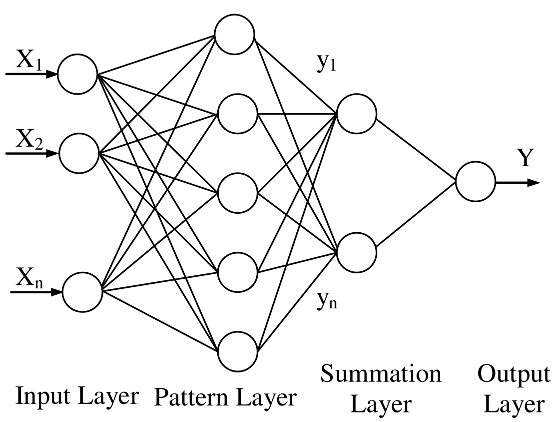

Fig. 5. General structure of a GRNN

The number of input units in input layer depends on the total number of the obtained parameters. The first layer is connected to the pattern layer and in this layer each neuron presents a training pattern and its output. The pattern layer is connected to the summation layer. The summation layer has two different types of summation, which are a single division unit and summation units. The summation and output layer together perform a normalization of output set. In training of network, radial basis and linear activation functions are used in hidden and output layers. Each pattern layer unit is connected to the two neurons in the summation layer, S and D summation neurons. S summation neuron computes the sum of weighted responses of the pattern layer. On the other hand, D summation neuron is used to calculate unweighted outputs of pattern neurons. The output layer merely divides the output of each S-summation neuron by that of each D-summation neuron, yielding the predicted value to an unknown input vector x as (Kim et al 2004);

$$Y_i' = \frac{\sum_{i=1}^{n} y_i . \exp[-D(x, x_i)]}{\sum_{i=1}^{n} \exp[-D(x, x_i)]} \tag{13}$$

$$D(x, x_i) = \sum_{k=1}^{m} (\frac{x_i - x_{ik}}{\sigma})^2 \tag{14}$$

y_i is the weight connection between the i^th^ neuron in the pattern layer and the S-summation neuron, n is the number of the training patterns, D is the Gaussian function, m is the number of elements of an input vector, x_k *and* x_{ik} are the k^th^ element of x *and* x_i, respectively, σ is the spread parameter, whose optimal value is determined experimentally.

4. Numerical Analysis

Natural frequencies for the first three modes of an elastically supported Timoshenko beam with 1, 3, 5, 8 and 10 attached masses are computed, initially, by TMM for parameters of f=0.1-0.25-0.5-0.75-0.99-0.999, $\overline{M}_i$=0.1-0.5-1-2.5-5-7.5-10, $\overline{J}_i$=0.1-0.5-1-5-10. m_i=0.32 kNs^2/m^2, L_i=1 m, EI=1353870 kNm^2, AG=3240000 kN, k=2.426, S_x=0.00743 m^3, A=0.04 m^2, I=0.006447 m^4 are the characteristics of the IPB profile beam used for the numerical analysis. The frequency values obtained for the beam with 1, 5 and 10 attached masses are used in training and testing phases whereas for the beam with 3 and 8 attached masses in the verification phase of GRNN.

According to Eq.(1), the relationship between the connection stiffness ($K_\theta L/EI$) and the fixity factor (f) is approximately linear when the fixity factor values are between 0.0 and 0.5 and nonlinear from 0.5 to unity as shown in Fig. 6. It can be seen from the graph that as the fixity factor approaches unity the curve increases asymptotically to infinity since the fixity factor of unity is used for theoretically ideal fixed support.

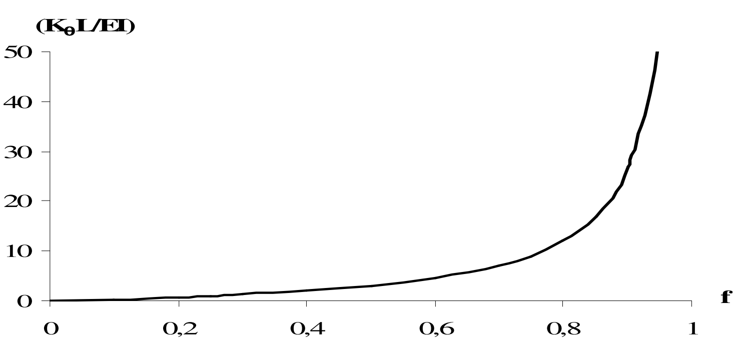

Fig. 6. Relationship between the connection stiffness ($K_\theta L/EI$) and the fixity factor (f)

4.1. The GRNN Model

The statistical parameters (i.e., minimum value; $x_{\min}$, maximum value; $x_{\max}$, mean; $\overline{x}$, standard deviation; s_x, skewness coefficient; c_{sx}) for the total data sets obtained by TMM for training/testing and verification phases are given in Table 1 and in Table 2.

Table 1. Statistical parameters for the beams with 1, 5 and 10 attached masses used in training/testing phase

		$x_{\min}$	$x_{\max}$	$\bar{x}$	s_x	c_{sx}
inputs	no. of attached masses	1	10	5.333	3.6847	0.1354
	dimensionless value of attached mass	0.1	10	3.8	3.542	0.5813
	dimensionless value of rotary inertia	0.1	10	3.32	3.7752	0.8759
	fixity factor	0.1	0.999	0.5982	0.3458	-0.1568
outputs	1. mode frequency	6	2614	322.0921	476.0394	2.2199
	2. mode frequency	78	6245	1169.2429	1532.6008	1.8918
	3. mode frequency	209	9293	2854.7825	3071.8198	0.7455

Table 2. Statistical parameters for the beams with 3 and 8 attached masses used in verification phase

		$x_{\min}$	$x_{\max}$	$\bar{x}$	s_x	c_{sx}
inputs	no. of attached masses	3	8	5.5	2.503	$2.13\text{x}10^{-17}$
	dimensionless value of attached mass	0.1	10	3.8	3.5434	0.582
	dimensionless value of rotary inertia	0.1	10	3.32	3.7767	0.877
	fixity factor	0.1	0.999	0.5982	0.3459	-0.157
outputs	1. mode frequency	9	593	126.9238	122.4172	1.5274
	2. mode frequency	113	2084	558.9024	432.282	1.3897
	3. mode frequency	287	4166	1113.031	812.11	1.6108

One of the most important steps in developing a satisfactory forecasting model is the selection of the input variables. The natural frequencies are affected by support condition. Rotational spring is used for the elastic support to model the general support conditions. Increases in spring coefficient values cause increases in frequencies. Fixity factor concept is used in the study to formulate elastic support behavior. Theoretically, zero for fixity factor value denotes a pinned support whereas infinity denotes a fixed support. Therefore, variation of fixity factor is considered one of the effective variables on frequency values.

The attached mass on the beam is determined as the second variable. The number and the value of the attached masses are directly related to frequency values of the beam. Increasing the number and the value of the attached masses decreases the frequency values. The third variable determined for the input parameter is the rotary inertia of the attached mass. An increase in the value of rotary inertia of the attached mass causes, also, a decrease in the frequency values. Generally in vibration problems, however, the models like in this study are the mathematical models that are formed to model more complex real systems. Therefore, determination of the value of the attached mass and of its rotary inertia is very hard and includes uncertainties. As a result, the nondimensional parameters for the attached mass and its rotary inertia are selected as the effective variables on vibration frequency.

It is evident that the training data sets should cover all the characters of the problem in order to get effective estimation. The obtained data is divided into three parts: training data set, testing data set and verification data set. The verification data set is consisting of the beam models with 3 and 8 attached masses. The training and testing data set include the beam models with 1, 5 and 10 attached masses. All data sets are obtained by TMM.

The frequency values of the elastically supported Timoshenko beam with 1, 3, 5, 8 and 10 attached masses are computed by TMM, and trained/tested for data of the beam with 1, 5 and 10 masses and estimated for data of the beam with 3 and 8 masses by GRNN. The comparison graphs of the frequency values obtained for the models with 1, 5 and 10 attached masses for the training phase are presented in Fig. 7.a, b and c respectively for the first, second and third modes. The graphs obtained for the testing phase are presented respectively for the first, second and third modes in Fig. 8.a, b, c for the model with 1 mass, in Fig. 9.a, b, c for the model with 5 masses, in Fig. 10.1, b, c for the model with 10 masses.

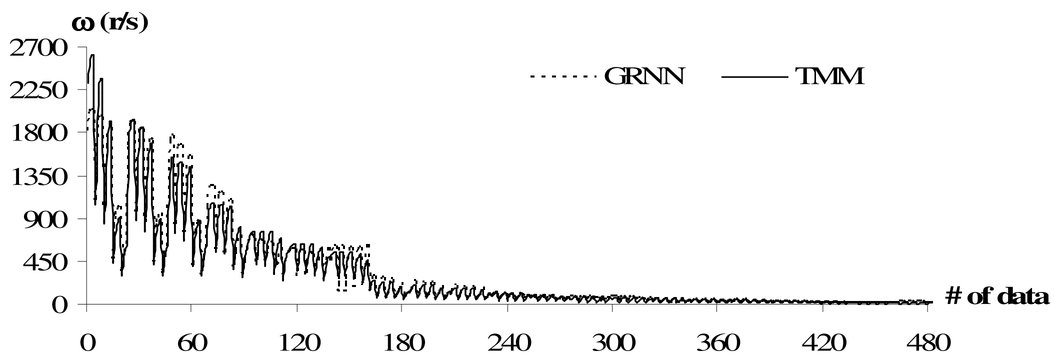

(a) first mode

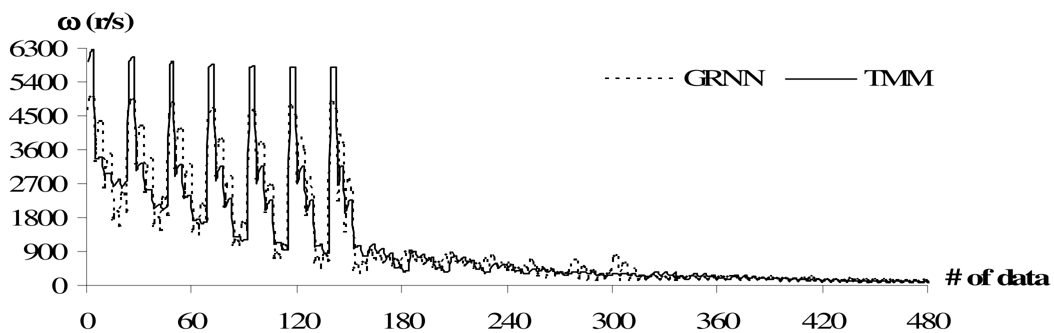

(b) second mode

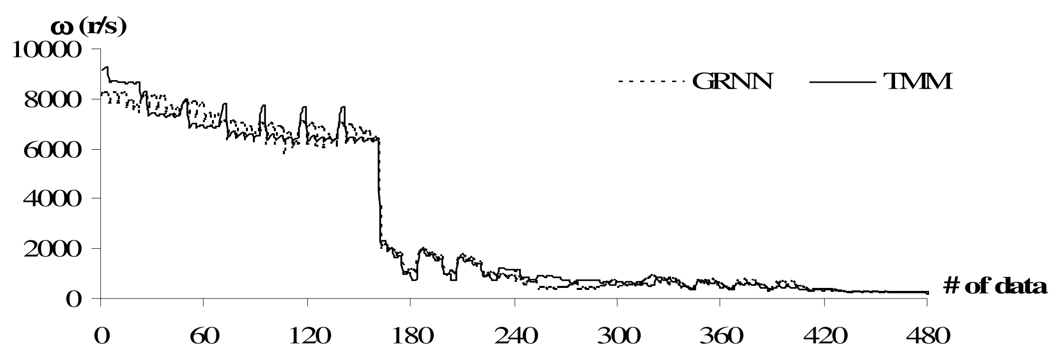

(c) third mode

Fig. 7. Frequency values obtained by TMM and by GRNN in training phase of the beam with 1, 5 and 10 attached masses

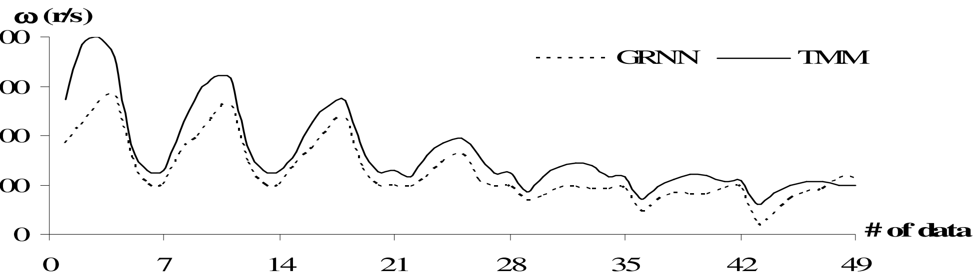

(a) first mode

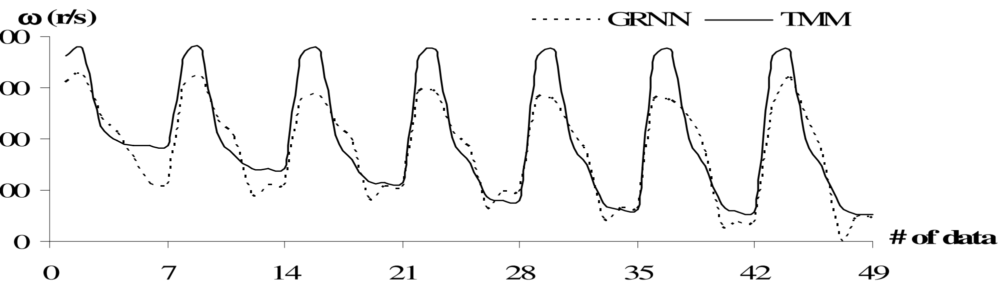

(b) second mode

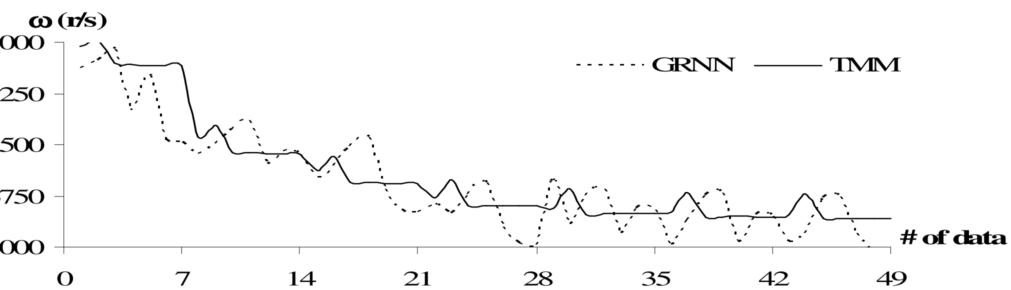

(c) third mode

Fig. .8 Frequency values obtained by TMM and by GRNN in testing phase of the beam with 1 attached mass

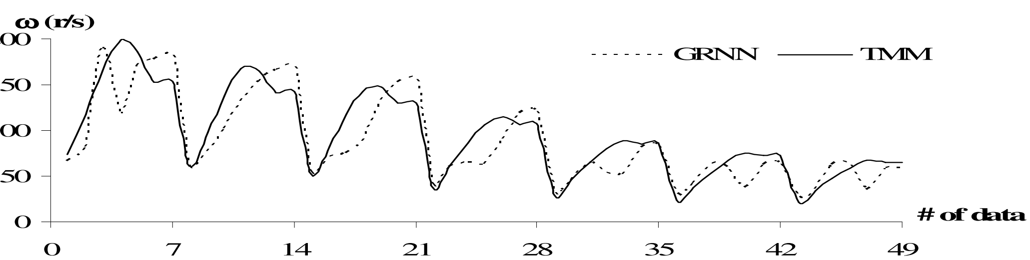

(a) first mode

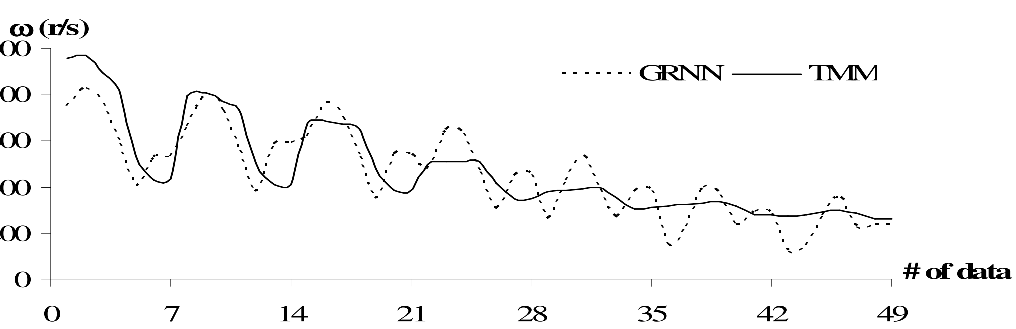

(b) second mode

(c) third mode

Fig. 9. Frequency values obtained by TMM and by GRNN in testing phase of the beam with 5 attached masses

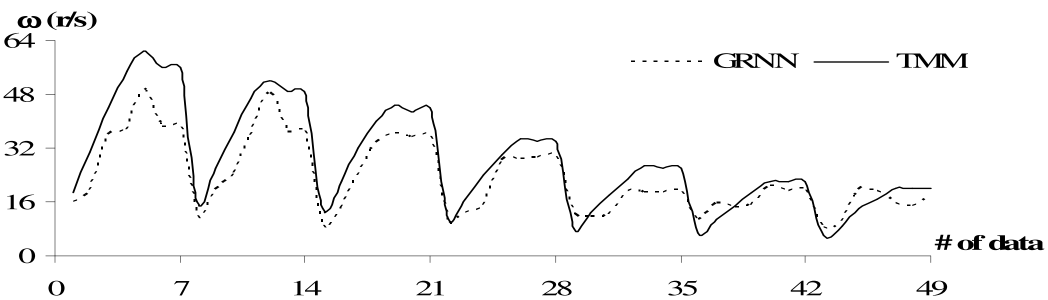

(a) first mode

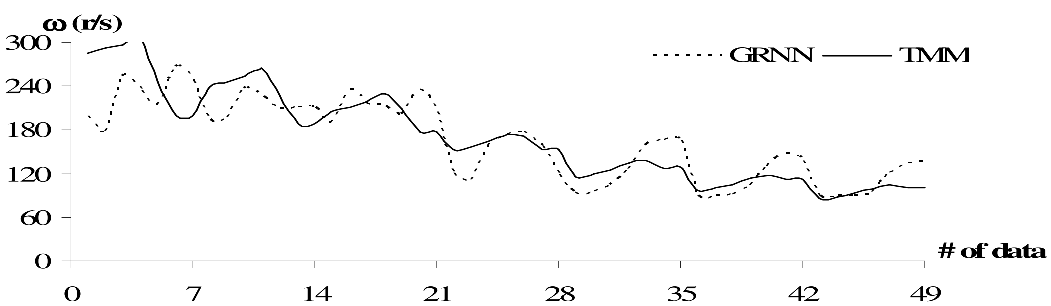

(b) second mode

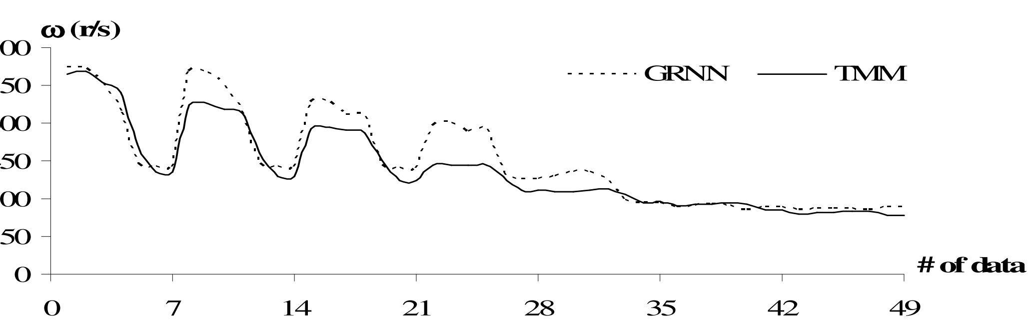

(c) third mode

Fig. 10. Frequency values obtained by TMM and by GRNN in testing phase of the beam with 10 attached masses

The performance of GRNN estimation model is given in Table 3 for training and in Table 4 for testing phase where the Correlation Coefficients (R) and the root mean squared errors (RMSE) are computed, respectively, from Eqs. (15.1) and (15.2).

$$R = \frac{\sum_{i=1}^{N}(Q_D - \overline{Q_D}).(Q_Y - \overline{Q_Y})}{\sqrt{\sum_{i=1}^{N}(Q_D - \overline{Q_D})^2.(Q_Y - \overline{Q_Y})^2}} \tag{15.1}$$

$$RMSE = \sqrt{\frac{\sum_{i=1}^{N}(Q_y - Q_D)^2}{N}} \tag{15.2}$$

where, Q_Y is the estimated frequency by GRNN, Q_D is the exact frequency obtained by TMM, $\overline{Q_y}$ is the average of the estimated frequencies, $\overline{Q_D}$ is the average of the exact frequencies, N is the number of data used in the corresponding phase of GRNN.

Table 3. The performance of the GRNN models in the training phase

No. of mode	No. of masses attached to beam	Correlation Coefficient R	Root Mean Square Error RMSE
1		0.9870	77.93
2	1, 5, 10	0.9630	406.94
3		0.9950	320.49

Table 4. The performance of the GRNN models in the testing phase

No. of mode	No. of masses attached to beam	Correlation Coefficient R	Root Mean Square Error RMSE
1	1	0.9592	247.6763
	5	0.8720	24.29
	10	0.9580	7.6125
2	1	0.9310	759.2383
	5	0.8383	111.1961
	10	0.8256	35.5934
3	1	0.8645	418.8416
	5	0.9420	162.6007
	10	0.9545	65.268

As it can be seen from Table 3, the correlation coefficients are so close to unity and it means with the Fig. 7 that an efficient training phase is achieved in GRNN. One can see, also for the testing phase, in Table 4 that the higher numbers of masses are attached to the beam the less root mean squared errors are obtained for the corresponding mode. In the Figs. 8, 9 and 10 the best fit between TMM and GRNN curves for the testing phase is achieved for the third mode; in addition, among the third mode graphs the beam with 10 attached masses gives the best fit.

The performance of GRNN estimation model is given in Table 5, and the frequency curves obtained using the data of beam with 3 and 8 attached masses are given in Figs 11 and 12, respectively, for verification phase. It can be seen from Table 5, as in the testing phase, that the higher numbers of attached masses are considered on the beam the less RMSE values are achieved for the corresponding mode.

Table 5. The performance of the GRNN models in the verification phase

No. of mode	No. of masses attached to beam	Correlation Coefficient R	Root Mean Square Error RMSE
1	3	0.9370	81.7266
	8	0.9218	15.6843
2	3	0.9199	170.4435
	8	0.8683	55.6108
3	3	0.8179	662.0744
	8	0.9390	100.304

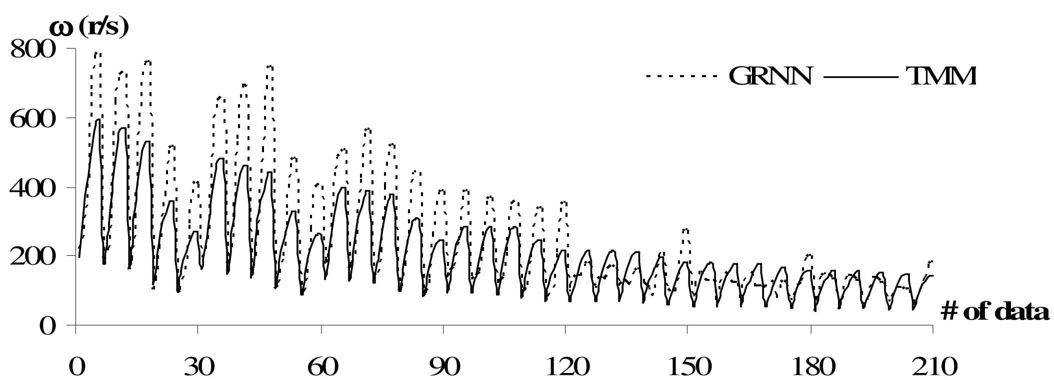

(a) first mode

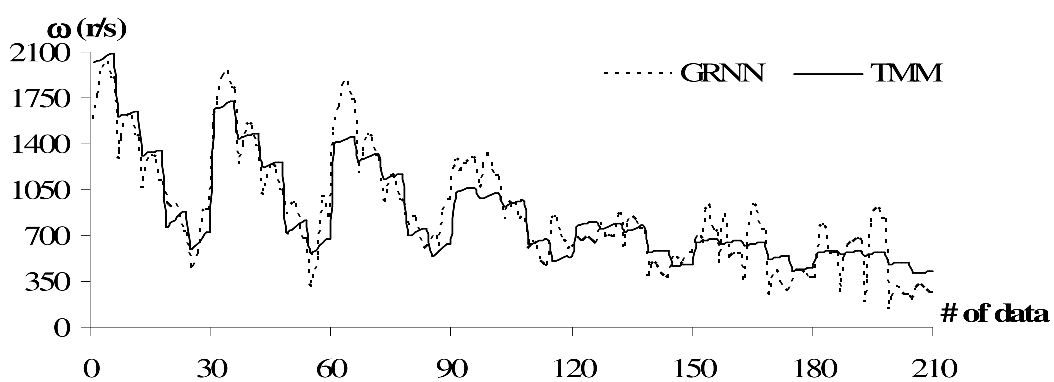

(b) second mode

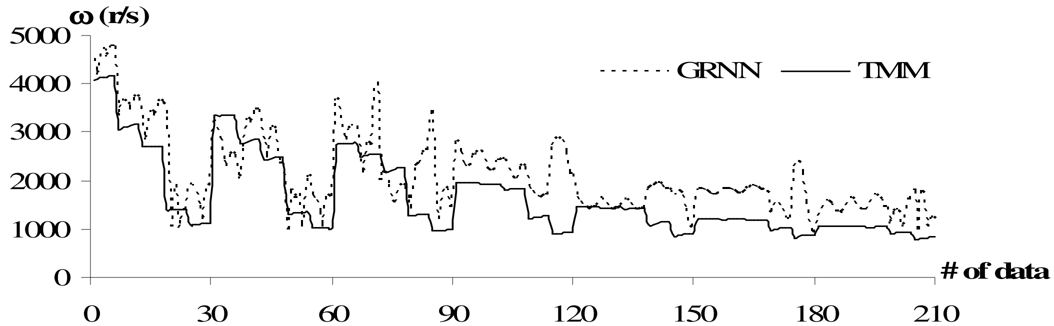

(c) third mode

Fig. 11. Frequency values obtained by TMM and estimated by GRNN in verification phase of the beam with 3 attached masses

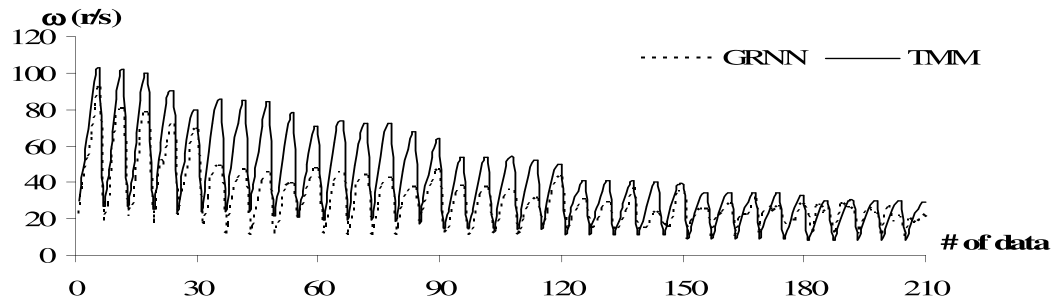

(a) first mode

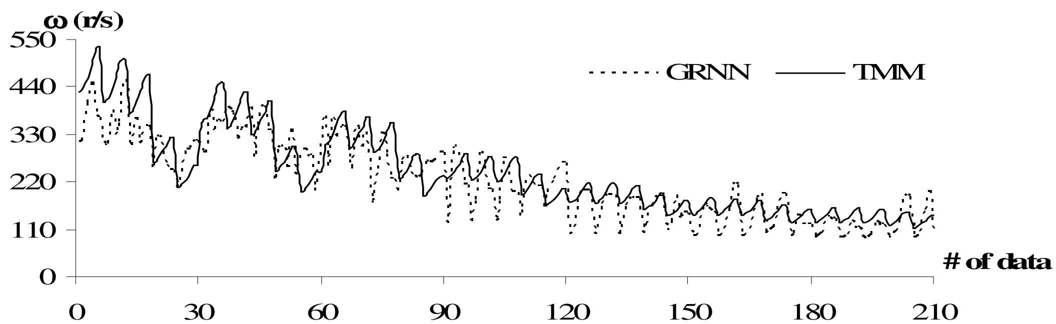

(b) second mode

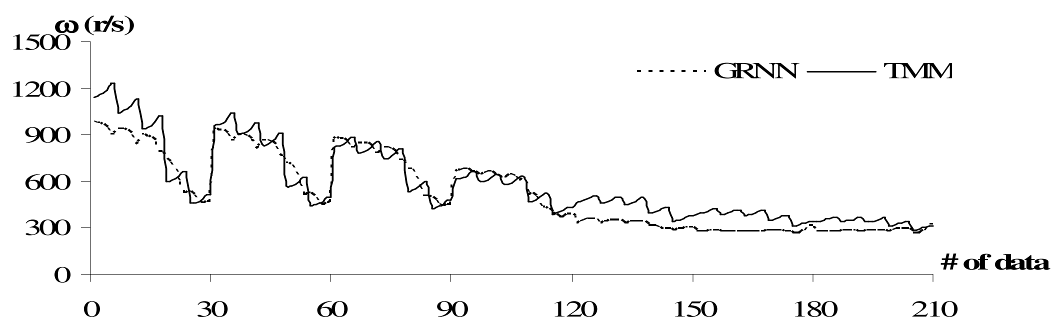

(c) third mode

Fig. 12. Frequency values obtained by TMM and estimated by GRNN in verification phase of the beam with 8 attached masses

5. Conclusions

In this study, elastically supported Timoshenko beam with attached masses is under consideration to obtain its free vibration natural frequencies using transfer matrix method and to estimate using neural network approach.

For one or two span models it is easy to obtain the frequency equation in explicit form by equating the determinant of coefficient matrix written according to boundary conditions of the entire system to zero, however, for large number of spans frequency equation will be extremely complex, therefore, the transfer matrix method will be more computationally efficient for these kind of models. In addition, another effective method –neural network approach- that reduces the computational effort and time is also used to obtain the free vibration frequencies of the model in the study.

The results of TMM and the GRNN models are compared in training, testing and verification sets; the comparison of the test sets with TMM is given in graphs, and the performance of the training, testing and verification phases of GRNN sets are given in the tables. From the comparing graphs in Fig. 7, it can be concluded that neural network approach gives very successful results in the training phase that are generally close to the values obtained from TMM. It is seen from performance tables that correlation coefficients of the training phase have the closest value to unity. RMSE value is rapidly decreasing as the number of attached mass is increasing both in the testing phase and in the verification phase; it means that neural network approach give better results for the beam with five attached masses than with one and for the beam with ten attached masses than with five. Thus, GRNN approach may give encouraging results for these kinds of models having great number of attached masses.

References

Allı, H., Uçar, A., & Demir Y. (2003). The solutions of vibration control problems using artificial neural networks. Journal of the Franklin Institute, 340, 307-325.

Bapat, C. N., & Bapat C. (1987). Natural frequencies of a beam with non-classical boundary conditions and concentrated masses. Journal of Sound and Vibration, 112, 177-182.

Cabrero, J. M., & Bayo E. (2005). Development of practical design methods for steel structures with semi-rigid connections. Engineering Structures, 27, 1125-1137.

Celikoglu H. B. (2006). Application of radial basis function and generalized regression neural networks in non-linear utility function specification for travel mode choice modeling. Mathematical and Computer Modeling, 44, 640–658.

Celikoglu, H. B., & Cigizoglu H. K. (2007). Public transportation trip flow modeling with generalized regression neural Networks. Advances in Engineering Software, 38, 71–79.

Cigizoglu, H. K., & Alp M. (2005). Generalized regression neural network in modelling river sediment yield. Advances in Engineering Software, 37, 63–68.

Esmailzadeh, E., & Ohadi A. R. (2000). Vibration and stability analysis of non-uniform Timoshenko beams under axial and distributed tangential loads. Journal of Sound and Vibration, 236, 443-456.

Ferreira, A.J.M., & Fasshauer G. E. (2006). Computation of natural frequencies of shear deformable beams .and plates by an RBF-Pseudospectral method. Computer Methods in Applied Mechanics and Engineering, 196, 134-146.

Gökdağ, H., & Kopmaz O. (2005). Coupled bending and torsional vibration of a beam with in-span and tip attachments. Journal of Sound and Vibration, 287, 591-610.

Hurty, W. C., & Rubinstein, M. F. (1964). Dynamics of structures. India: Prentice Hall, (Chapter 5).

Karami, G., Malekzadeh, P., & Shahpari S. A. (2003). A DQEM for vibration of shear deformable nonuniforms beams with general boundary conditions. Engineering Structures, 25, 1169-1178.

Karlık, B., Özkaya, E., Aydın, S., & Pakdemirli M. (1998). Vibrations of a beam-mass systems using artificial neural networks. Computers and Structures, 69, 339-347.

Kim, B., Lee, D. W., Parka, K. Y., Choi, S. R., & Choi S. (2004). Prediction of plasma etching using a randomized generalized regression neural network. Vacuum, 76, 37–43.

Lee, U., Kim, J., & Oh H. (2004). Spectral analysis for the transverse vibration of an axially moving Timoshenko beam. Journal of Sound and Vibration, 271, 685-703.

Lin, H. P., & Chang S.C. (2005). Free vibration analysis of multi-span beams with intermediate flexible constraints. Journal of Sound and Vibration, 281, 155-169.

Low K. H. (1991). A comprehensive approach for the eigenproblem of beams with arbitrary boundary conditions. Computers and Structures, 39, 671-678.

Özkaya, E., & Pakdemirli M. (1999). Non-linear vibrations of a beam-mass system with both ends clamped. Journal of Sound and Vibration, 221, 491-503.

Özkaya E. (2002). Non-linear transverse vibrations of a simply supported beam carrying concentrated masses. Journal of Sound and Vibration, 257, 413-424.

Özkaya, E., & Öz H. R. (2002). Determination of natural frequencies and stability regions of axially moving beams using artificial neural networks method. Journal of Sound and Vibration, 252, 782-789.

Posiadala B. (1997). Free vibrations of uniform Timoshenko beams with attachments. Journal of Sound and Vibration, 204, 359-369.

Ramadhas, A. S., Jayaraja, S., Muraleedharan, C., & Padmakumar K. (2006). Artificial neural networks used for the prediction of the cetane number of biodiesel. Renewable Energy, 31, 2524–2533.

Rao, G. V., Saheb, K. M., & Janardhan G. R. (2006). Fundamental frequency for large amplitude vibrations of uniform Timoshenko beams with central point concentrated mass using coupled displacement field method. Journal of Sound and Vibration, 298, 221-232.

Ruta P. (2006). The application of Chebyshev polynomials to the solution of the nonprismatic Timoshenko beam vibration problem. Journal of Sound and Vibration, 296, 243-263.

Salarieh, H., & Ghorashi M. (2006). Free vibration of Timoshenko beam with finite mass rigid tip load and flexural-torsional coupling. International Journal of Mechanical Sciences, 48, 763-779.

Thomson W. T. (1981). Theory of vibration with application. USA: Prentice Hall, (Chapter 7).

Tuma J. J., & Cheng, F. Y. (1983). Theory and Problems of Dynamic Structural Analysis: Schaum's Outline Series. USA: McGraw-Hill, Inc., (Chapter 7).

Wu, J.S., & Chen D.W. (2001). Free vibration analysis of a Timoshenko beam carrying multiple spring-mass systems by using the numerical assembly technique. International Journal for Numerical Methods in Engineering, 50, 1039-1058.

Wu, J. S., & Chiang L. K. (2004) Free vibration of solid and hollow wedge beams with rectangular or circular cross-sections and carrying any number of point masses. International Journal for Numerical Methods in Engineering, 60, 695-718.

Wu J. J. (2006). Use of equivalent mass method for free vibration analysis of a beam carrying multiple two-dof spring-mass systems with inertia effect of the helical springs considered. International Journal for Numerical Methods in Engineering, 65, 653-678.